Journal of Biomechanics 177 (2024) 112402

Contents lists available at ScienceDirect

Journal of Biomechanics

journal homepage: www.elsevier.com/locate/jbiomech

Exploring healthy knee kinematic phenotypes obtained through dynamic CT imaging: A cluster analysis study

E.H.S. Teule [a,b,*], S.A.W. van de Groes [a], G. Hannink [c], N. Verdonschot [a,d], D. Janssen [a]

[a] Radboud University Medical Center, Orthopaedic Research Laboratory, Nijmegen, Netherlands (the)
[b] Radboud University Medical Center, Department of Plastic Surgery, Nijmegen, Netherlands (the)
[c] Radboud University Medical Center, Department of Medical Imaging, Nijmegen, Netherlands (the)
[d] University of Twente, Laboratory of Biomechanical Engineering, Enschede, Netherlands (the)

ARTICLE INFO

Keywords:
Dynamic CT
K-means clustering
Knee kinematics
Healthy participants
Kinematic phenotypes

ABSTRACT

Dynamic Computed Tomography (CT) emerges as a pivotal imaging modality for the assessment of knee joint kinematics. However, integrating dynamic CT into clinical practice necessitates a thorough understanding of healthy knee kinematics, as large variation in kinematics has been described within healthy populations. Therefore, this study aims to identify and describe healthy phenotypes with homogenous knee kinematics using a clustering approach. A total of 120 healthy knees from 64 participants underwent dynamic CT scanning during knee extension and flexion. Eight tibiofemoral (TF) and patellofemoral kinematic parameters were extracted, after which K-means clustering was applied to identify homogenous kinematic clusters. Kinematic phenotypes were obtained by calculating the median and interquartile range (IQR) for all kinematic parameters per cluster. Two distinct clusters were found, comprising 53 (Cluster 1) and 67 (Cluster 2) knees. Statistically significant differences between the clusters were found in six out of eight kinematic parameters. The most notable differences were observed in TF rotations, with cluster 1 exhibiting a greater amount of internal and adduction rotation of the tibia compared to cluster 2. The two kinematic phenotypes provide new insights into the nuanced variation within a healthy cohort and can serve as reference for future studies evaluating pathological kinematic phenotypes using dynamic CT.

1. Introduction

Dynamic Computed Tomography (CT) emerges as a pivotal imaging modality in musculoskeletal research, facilitating comprehensive assessment of joint kinematics (Wong et al., 2022). Specifically for the knee joint, this technique enables evaluation of pathologies such as patellofemoral (PF) instability during knee movement (Buzzatti et al., 2021; Wong et al., 2022). Dynamic imaging provides additional insights into tibiofemoral (TF) and PF kinematics compared to static imaging (Dandu et al., 2022; Rosa et al., 2019; Yu et al., 2019), and recent studies have identified distinct patellar tracking patterns in individuals with PF instability (Esfandiarpour et al., 2018; Rosa et al., 2019; Shen et al., 2021; Tanaka et al., 2016). Integrating dynamic CT into clinical practice necessitates a thorough understanding of healthy knee kinematics, which can be used to compare patient-specific knee kinematics with normative data (Yu et al., 2019).

Research on healthy knee kinematics shows considerable variability in TF and PF kinematics (Clement et al., 2018; Gale & Anderst, 2020; Yu et al., 2019). Anatomical differences and gender affect this variability, as individuals with greater valgus alignment (typically women) exhibit an increased tibial abduction movement (Barrios et al., 2016; Clement et al., 2018). Nonetheless, the full spectrum of variation in knee kinematics remains incompletely understood. Bridging this gap requires innovative approaches, and machine learning techniques, especially clustering analysis, are valuable tools for characterizing kinematic phenotypes in vast amounts of data (Abid et al., 2019). Clustering analysis classifies data into homogenous clusters by maximizing the similarity within and the separation between clusters. Recent studies applying clustering approaches have identified distinct kinematic phenotypes, highlighting the diversity in healthy knee motion during gait (Clement et al., 2018; Mezghani et al., 2021; Zgolli et al., 2018;). However, quantitative instrumented gait analysis may pose challenges

* Corresponding author at: Orthopaedic Research Lab, Radboud University Medical Center, Geert Grooteplein Zuid 10, 6525 GA Nijmegen, Netherlands (the).
E-mail addresses: erin.teule@radboudumc.nl (E.H.S. Teule), sebastiaan.vandegroes@radboudumc.nl (S.A.W. van de Groes), gerjon.hannink@radboudumc.nl (G. Hannink), nico.verdonschot@radboudumc.nl (N. Verdonschot), dennis.janssen@radboudumc.nl (D. Janssen).

https://doi.org/10.1016/j.jbiomech.2024.112402
Accepted 29 October 2024
Available online 1 November 2024
0021-9290/© 2024 The Author(s). Published by Elsevier Ltd. This is an open access article under the CC BY license (http://creativecommons.org/licenses/by/4.0/).

in clinical settings due to logistical constraints, whereas dynamic CT is a clinically relevant tool to quantify knee kinematics that can be performed directly in outpatient clinical setting.

Before dynamic CT can be implemented for knee pathology assessment, it is crucial to understand the variation in healthy knee kinematics. Dunning et al. used dynamic CT to extract knee kinematics from 100 healthy individuals, revealing substantial variation and suggesting different kinematic phenotypes even among healthy individuals (Dunning et al., 2023). This may complicate distinguishing patients and healthy participants at an individual level. It is essential to identify and understand these healthy kinematic phenotypes in order to better differentiate between PF instability and healthy knee movement. Consequently, this study aims to identify and describe healthy knee kinematic phenotypes using dynamic CT data and clustering analysis.

2. Methods

This study used bilateral CT data from 100 healthy participants (i.e. 200 knees), obtained between 2020 and 2021. Participants were included in a 3:7 male/female ratio (70 % female) and were aged 18–35, representing a healthy control group for patients with PF instability (Fithian et al., 2004; Zheng et al., 2022). Institutional review board approval was obtained (NL72784.091.20) and all participants provided written informed consent for secondary use of their data. Participants had no history of knee pathologies, previous trauma, or surgery on the knees. Exclusion criteria included functional or congenital knee disorders, as well as visually diagnosed varus or valgus malalignment. Fig. 1 provides an overview of the methods section.

2.1. CT scanning protocol

All participants underwent CT scanning of both knees, as previously described by Dunning et al. (Dunning et al., 2023). In short, the scanning protocol consisted of a high-resolution static CT scan (Aquilion ONE; Canon Medical Systems) of both knees with the participant in supine position (field of view: 50 cm; mean voxel size: 0.71 × 0.71 × 0.80 mm). The participant was then positioned at the end of the scanner table in a semi-seated position, with their knees in 90° flexion. During a 10 s dynamic protocol, participants were asked to move both legs from this position to full knee extension and back to 90° of knee flexion (Fig. 2). During dynamic scanning, 41 dynamic CT scans of the knee joint at different flexion angles were obtained (field of view: 16 cm; mean voxel size: 0.98 × 0.98 × 0.50 mm). The total radiation dose was 0.08 mSv.

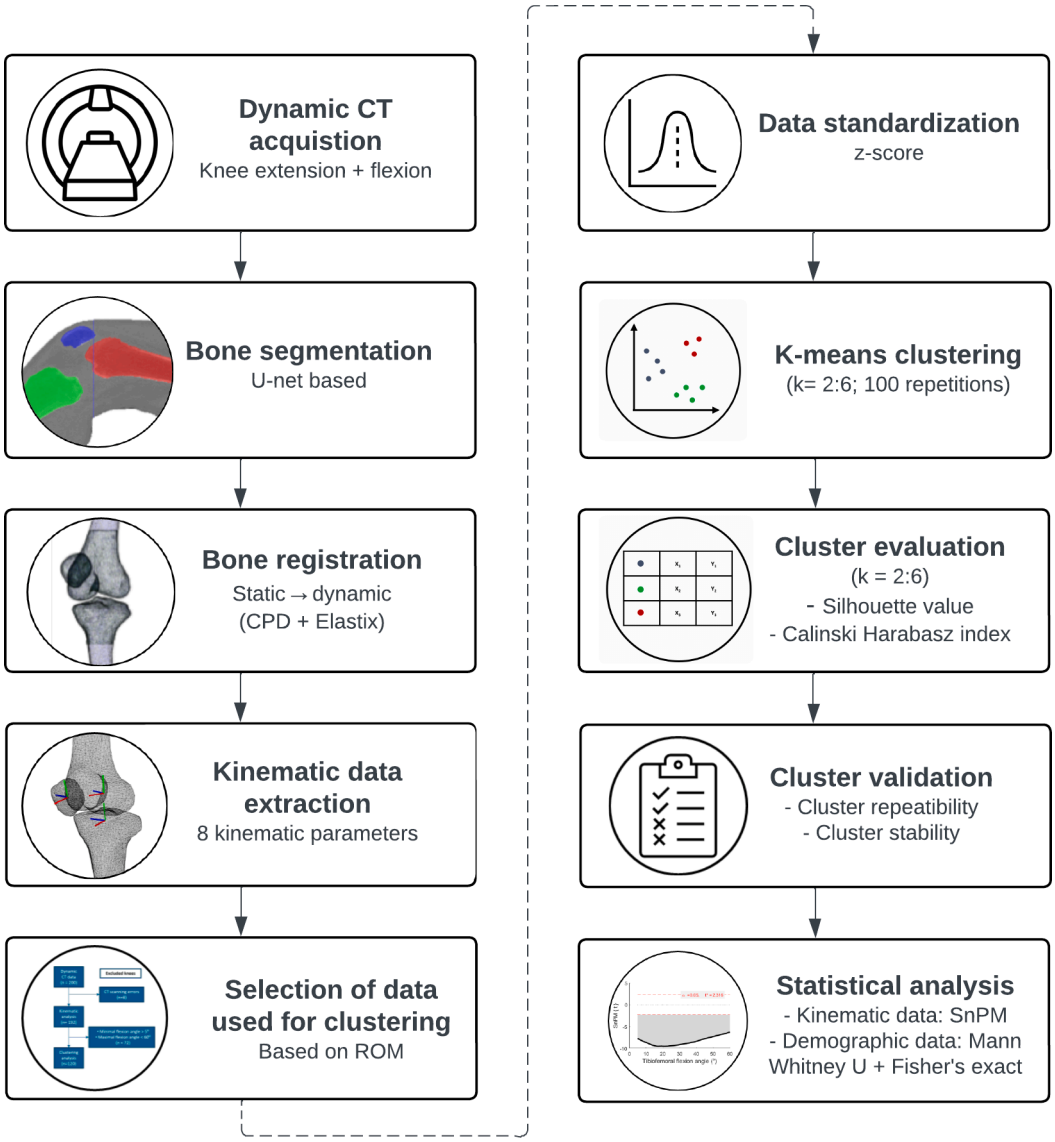

Fig. 1. Overview of all data analysis steps performed in this study. CPD: Coherent Point Drift; ROM: Range of Motion; SnPM: Statistical non-Parametric Mapping.

Fig. 2. Overview of scanning procedure with corresponding CT images. a) high-resolution static scan of the lower extremity, performed with the participant in supine position. b + c) dynamic scan acquisition while the participant is positioned at the end of the scanner table with an angled pillow in the popliteal fossa. The participant is instructed to perform full extension and flexion of both knees in 10 s.
Figure reproduced from our previous publication. (Dunning et al., 2023)

2.2. Quantification of tibiofemoral and patellofemoral kinematics

After image acquisition, the femur, patella and tibia were automatically segmented using a U-net algorithm (Li et al., 2018). Segmented masks were converted to 3D surface meshes in MATLAB (R2022b; MathWorks) and smoothed to improve mesh quality. The tibial tuberosity-trochlear groove distance was automatically measured in the static CT scan using a validated method described by Chen et al. (Chen et al., 2020). Bone meshes of the static scan were registered onto corresponding meshes of dynamic scans using point cloud (Coherent Point Drift) and intensity-based registration (Elastix 5.0.1). Registration accuracy was within 2° and 3 mm for rotations and translations, respectively (Adachi et al., 2023; Dunning et al., 2023). Subsequently, coordinate systems (CS) were calculated in bones from the static scan (femur, tibia and patella) and transformed to corresponding bones from dynamic scans, as explained in detail by Dunning et al. (Dunning et al., 2022; Miranda et al., 2010). From these CS, TF and PF kinematics were quantified using Grood & Suntay's description, with tibia and patella rotations calculated relative to the femur (Grood & Suntay, 1983). TF anterior-posterior (AP) translation was assessed as medial and lateral femoral rollback with respect to the tibia and relative to full knee extension, in other words, rollback at the smallest TF flexion angle was considered zero. Detailed explanations can be found in Dunning et al. (Dunning et al., 2023). The final kinematic output included eight parameters, plotted against the TF flexion angle: adduction / abduction rotation (°), internal / external rotation (°), medial and lateral femoral rollback (mm) (tibiofemoral joint); and flexion (°), rotation (°), tilt (°) and mediolateral translation (mm) (patellofemoral joint). All parameters were interpolated for every degree of knee flexion to allow for comparison between participants, and split into a knee flexion and an extension movement. In contrast to the approach of Dunning et al. (Dunning et al., 2023), rotational and translational offsets were not negated at the smallest TF flexion angle, except for medial and lateral femoral rollback. As the aim of this paper was to identify kinematic phenotypes within a healthy population, we decided to refrain from correcting for any anatomical variations within the dataset. The resulting healthy kinematic dataset was highly comparable to other studies reporting healthy knee kinematics, as detailed in Dunning et al. (Dunning et al., 2023).

2.3. Data preparation for clustering

Out of the initial 200 knees examined, eight knees from four participants were excluded due to CT scanning errors, such as anincorrect field of view. For the remaining knees, varying ranges of knee motion were observed, caused by the unrestricted movement permitted in the CT scanner. To ensure clinical relevance, knees were only included if they approached full extension (≤5°) and achieved a flexion angle of at least 60° during dynamic CT scanning, leading to the exclusion of an additional 72 knees from 40 participants (Fig. 3). Subsequently, the remaining 120 knees were combined into one dataset, consisting of 120

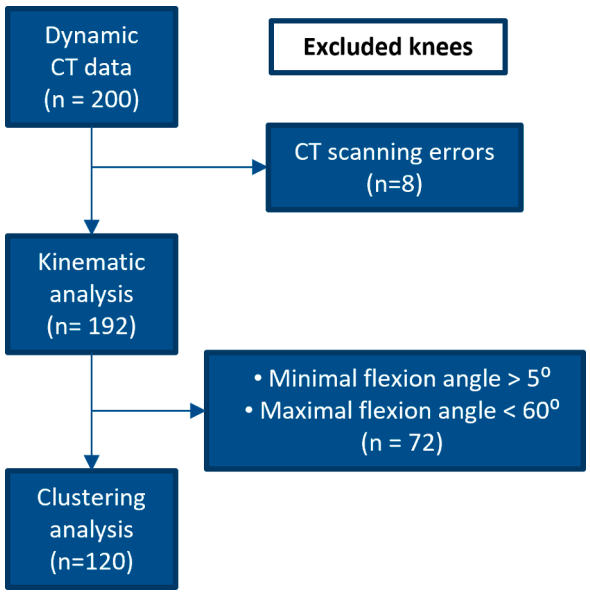

Fig. 3. Flowchart showing the reasons for exclusion of knees for clustering analysis.

rows (knees) and 952 columns, representing eight kinematic parameters measured at 56 angles during flexion (5°-60°) and 63 angles during the extension movement (67°-5°). Parameters were ordered consistently for every knee in the dataset. Each knee was assessed separately for the clustering algorithm, thus, both knees of the same participant could be assigned to different clusters. To mitigate the potential influence of outliers on clustering analysis, all parameters were standardized to z-scores (mean = 0; SD = 1). Following this standardization, outliers (|z-score| > 3) were identified for every kinematic parameter at every flexion angle. As none of the outliers affected clustering output, all outliers could be disregarded.

2.4. Clustering algorithm

K-means clustering was implemented to assign healthy knees into different clusters based on homogenous knee kinematics. This unsupervised machine learning technique iteratively partitions datapoints (knees) into a predetermined number of clusters (*k*) by minimizing the within-cluster sum of squared Euclidean distances to cluster centroids (Abiodun et al., 2023; MacQueen, 1967). Initially, cluster centroids were randomly seeded, potentially leading to local instead of global optima. To address this, 100 clustering repetitions with randomized starting centroids were conducted in each clustering process. The repetition yielding the lowest sum of squared Euclidean distances was selected as optimal allocation.

As K-means clustering requires the number of clusters as input, the

optimal number of clusters (k) was assessed by evaluating two cluster quality metrics, similar to methods proposed by Mezghani et al. and Petersen et al. (Mezghani et al., 2021; Petersen et al., 2022). The silhouette value (SV) compares cluster cohesion to cluster separation, with values ranging from −1 to 1. A higher value indicates better clustering, while negative values suggest misallocation of datapoints (Rousseeuw, 1987). The Calinski-Harabasz index (CH) quantifies the ratio of within-cluster to between-cluster dispersion, with higher values indicating better performance (Caliński & Harabasz, 1974). Both metrics were assessed for 2 to 6 clusters, as more than six clusters were deemed clinically irrelevant. The optimal number of clusters was chosen based on both quality metrics and clinical interpretability of the clusters.

2.5. Cluster validation

K-means clustering was applied to the kinematic dataset using the optimal number of clusters (k), and subsequently kinematic phenotypes were determined by computing the median and interquartile range (IQR) per cluster for all kinematic parameters. The resultant clustering output was validated by assessing cluster repeatability and stability. Cluster repeatability was determined by iteratively repeating the clustering process 100 times and comparing all allocation outputs. Cluster stability was evaluated by performing 100 clustering processes using a randomly selected subset comprising 100 knees of the original dataset. Following each clustering iteration, the allocation output was compared to the ground truth, represented by the defined cluster partitioning in the original dataset. The Adjusted Rand Index (ARI), a metric ranging between −1 and 1 quantifying agreement between two partitions, was used to assess both cluster repeatability and stability (Santos & Embrechts, 2009). Interpretation of ARI values was as follows: <0.65: poor agreement, <0.8 moderate agreement, <0.9: good agreement, and =>0.9: excellent agreement.

2.6. Statistical analysis

Continuous demographic participant characteristics were assessed for normality; as they did not adhere to a normal distribution, comparisons between clusters were conducted using Mann-Whitney U tests for continuous variables and Fisher's exact tests for binary categorical variables. Differences in knee joint kinematics between clusters were assessed using open-source software one-dimensional Statistical Parametric Mapping (SPM) for MATLAB (spm1d.org, version M.0.4.10). SPM allows for statistical testing along a 1D continuum (e.g. time series or kinematic trajectories) to detect differences. SPM incorporates random field theory to determine the significance threshold, thereby mitigating bias and enhancing the sensitivity and robustness of the analysis (Pataky et al., 2013; Pataky et al., 2015). Statistical non-Parametric Mapping (SnPM) was employed for cluster comparison given the non-normal distribution of the kinematic data. Statistical significance was set at $p < 0.05$ for all tests conducted.

Table 1
Cluster quality assessment for 2 to 6 clusters. The bold numbers indicate the highest cluster quality value for that metric.

Nr of clusters	2	3	4	5	6
Silhouette value	0.243	**0.260**	0.217	0.199	0.216
Calinski-Harabasz	**21.69**	18.78	17.00	15.42	14.62

3. Results

A total of 120 knees (62 right, 52 %) from 64 participants (53 female, 83 %) were included. The average age was 24 years (IQR 22–27) and BMI was 22.0 kg/m^2 (IQR 20.8–23.8) (Table 2). Cluster quality was assessed for 2 to 6 clusters (Table 1). The SV favored $k = 3$ for optimal clustering performance, while the CH suggested $k = 2$. Visual inspection of both solutions revealed that in the $k = 3$ solution, the third cluster closely resembled the kinematics of one of the other clusters and did not represent a distinct kinematic phenotype. In contrast, the $k = 2$ solution provided two clearly distinguishable kinematic phenotypes for almost all kinematic parameters. Combined with the minimal difference in SV between $k = 2$ and $k = 3$, this supported the selection of $k = 2$ as the optimal number of clusters. Cluster repeatability for $k = 2$ showed 100 % consistency in cluster allocation across 100 clustering processes. Additionally, cluster stability assessment resulted in a mean ARI of 0.93 (SD 0.06), indicating stable clusters for $k = 2$.

The final K-means clustering resulted in two distinct clusters, comprising 53 and 67 knees, respectively. Cluster 1 had 53 knees from 35 participants, and cluster 2 comprised 67 knees from 39 participants. 82 % of the participants had both knees allocated to the same cluster. Statistically significant demographic differences between the clusters were found for gender and height; Cluster 1 comprised 14.1 % more males (95 % CI: 0.4–27.8) and participants were on average 5 cm taller (95 % CI: 2.0–7.0) than cluster 2 (Table 2). Furthermore, statistically significant differences throughout (part of) the knee motion were found for all parameters except lateral and medial femoral rollback. Fig. 4 compares the two clusters for the four clinically most important kinematic parameters: TF internal / external rotation, TF abduction / adduction rotation, PF tilt and PF translation. Detailed results for the other parameters can be found in the supplementary materials (Suppl. Figure I). Notably, flexion and extension movements exhibited analogous patterns across all kinematic parameters for both clusters.

Cluster 1

This cluster (n = 53) predominantly consisted of female knees (75 %) and the majority of knees were right-sided (57 %). Participants in cluster 1 were 5 cm taller (95 % CI: 2.0–7.0) than those in cluster 2, likely influenced by the higher proportion of males in this cluster. Knees in this cluster exhibited more tibial adduction between 20°-70° of knee flexion, and the tibia was more internally rotated throughout the whole knee movement. In terms of PF kinematics, knees in this cluster demonstrated reduced lateral tilt and lateral translation throughout the whole knee movement (Fig. 4), and relatively less patellar flexion and medial patellar rotation (Suppl. Figure I).

Table 2
Demographic and knee characteristics in the two clusters (median (interquartile range) for all continuous variables). CI: confidence interval; BMI: body mass index; TTTG: tibial tuberosity – trochlear groove.

Characteristic	All knees (n = 120)	Cluster 1 (n = 53)	Cluster 2 (n = 67)	P-value	Difference between clusters (95 % CI)
Left knees, *n* (%)	58 (48 %)	23 (43 %)	35 (52 %)	0.363	8.8 (−9.1 – 26.8)
Females, *n* (%)	100 (83 %)	40 (75 %)	60 (90 %)	0.050	14.1 (0.4 – 27.8)
Age (years)	24.0 (22.0 – 27.0)	25.0 (22.0 – 27.0)	23.0 (22.0 – 26.0)	0.170	1.0 (0.0 – 2.0)
Weight (kg)	65.0 (60.3 – 72.0)	66.0 (62.0 – 73.0)	64.0 (60.0 – 72.0)	0.236	1.5 (−1.0 – 5.0)
Height (cm)	170.0 (167.0 – 176.0)	174.0 (169.0 – 179.5)	169.0 (167.0 – 174.0)	0.002	5.0 (2.0 – 7.0)
BMI (kg/m^2)	22.0 (20.8 – 23.8)	22.0 (20.9 – 23.3)	22.0 (20.8 – 24.1)	0.399	−0.4 (−1.2 – 0.5)
TTTG distance (mm)	12.6 (10.3 – 14.4)	12.0 (9.7 – 14.2)	13.0 (10.7 – 14.5)	0.116	−0.9 (−2.2 – 0.2)

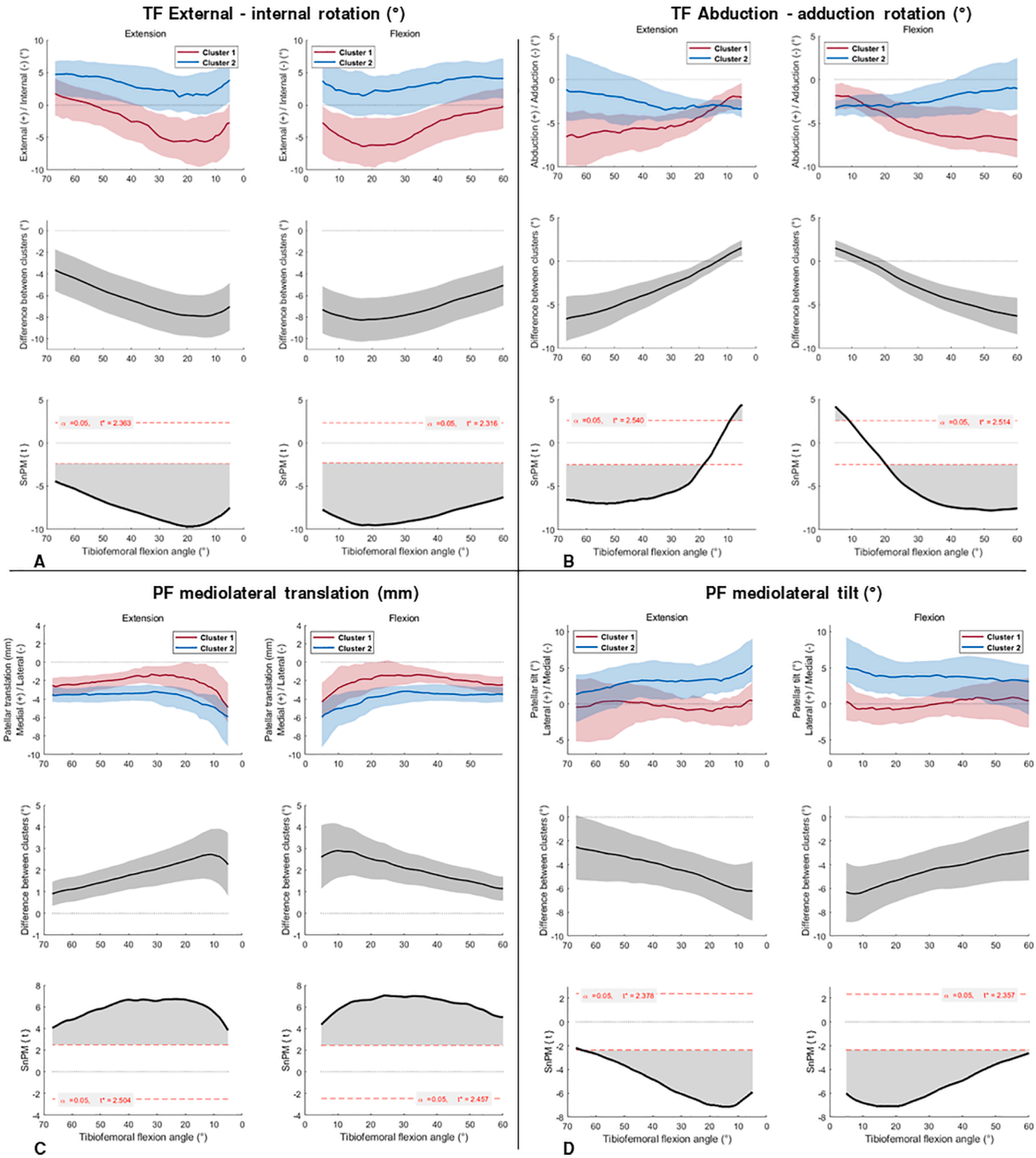

Fig. 4. Clustering results for four kinematic parameters during knee extension and flexion. A, B, C, and D: Top row: Kinematic phenotypes (median and interquartile range) of both clusters. Middle row: Average differences and 95% confidence interval between the two clusters. Bottom row: SnPM results indicating the t* threshold for significance (red dotted line) and the calculated test statistic (t; bold black line). Grey areas represent statistically significant differences between the two clusters. TF: Tibiofemoral; PF: Patellofemoral; SnPM: Statistical non-Parametric Mapping. (For interpretation of the references to colour in this figure legend, the reader is referred to the web version of this article.)

Cluster 2

This cluster consisted of 67 knees and comprised primarily female (90 %) and left knees (52 %). Knees in cluster 2 exhibited relatively increased tibial abduction between 20°-70° of knee flexion, and greater external rotation of the tibia throughout the entire movement. For PF kinematics, this cluster exhibited more pronounced lateral patellar tilt and lateral translation throughout the knee movement (Fig. 4). Furthermore, the patella demonstrated increased medial rotation and greater patellar flexion (Suppl. Figure I).

4. Discussion

This study characterized healthy knee kinematics obtained from dynamic CT imaging using a K-means clustering approach, and identified two distinct kinematic phenotypes. The two clusters show statistically significant differences in 6 out of 8 kinematic parameters, both from TF and PF kinematics. These findings demonstrate the variability in

healthy knee motion, underscoring the importance of personalized approaches in diagnostics and treatment planning for knee pathology. Despite similarities in age, weight, and BMI between the clusters, statistically significant differences were found in gender and height. Specifically, cluster 1 comprised 14.1 % more males (95 % CI: 0.4–27.8) and participants were on average 5 cm taller (95 % CI: 2.0–7.0) compared to cluster 2.

When comparing kinematic phenotypes between the two clusters, notable differences primarily appear in internal/external and adduction/abduction rotation of the tibia (Fig. 4, A and B). Knees in cluster 1 demonstrate greater internal tibia rotation and increased tibial adduction. The latter may result from the higher number of male knees in this cluster, as males typically exhibit more tibial adduction during gait compared to females (Clement et al., 2018). However, due to the limited number of male knees in this study (n = 20, 17 %), further research involving a larger cohort of male knees is required. Furthermore, knees in cluster 1 exhibit almost no lateral patellar tilt and less lateral translation during knee flexion (Fig. 4, C and D). This is consistent with their more internally rotated tibia, as increased lateral patellar tilt correlates with tibial external rotation (Lin et al., 2008). Conversely, knees in cluster 2 demonstrate relatively more external tibia rotation, increased lateral patellar tilt, and greater lateral patellar translation, along with relatively more tibial abduction during 20°-70° of knee flexion. This indicates that within the healthy population, asymptomatic knee movement with relatively more lateral patellar tilt and translation can occur. Remarkably, adduction/abduction rotation does not differ between clusters near full extension (10°-20°). The screw home mechanism is observed in both clusters as a change in motion pattern towards greater external tibial rotation and increased lateral patellar tilt near extension (5°-10°). This phenomenon is particularly pronounced in cluster 1. Both clusters demonstrate greater lateral than medial femoral rollback, attributable to medial pivoting of the knee joint (Pinskerova et al., 2004). No statistically significant differences in femoral rollback between clusters were found, possibly due to the measurement method. As femoral rollback was measured as AP translation and set to zero in full extension, potential differences in starting position and orientation of the CS among participants were negated. To justify the sample sizes used in this study, a post hoc power analysis was conducted using power1d software (Pataky, 2017). This analysis determined that a minimum of 43 knees per cluster is required to adequately detect between-cluster differences up to 2 (mm or degrees), assuming standard deviations of 4, with a statistical power of 0.8 and $\alpha = 0.05$. Since the identified clusters in this study consisted of 53 and 67 knees, the sample sizes were sufficient.

No previous studies have analyzed healthy kinematic clusters using dynamic CT imaging, making direct comparison of our results challenging. However, clustering analysis on gait patterns in healthy knees has been conducted. Mezghani et al. identified three clusters in 150 healthy knees based on TF rotations, differing primarily in adduction/abduction and external/internal tibial rotation (Mezghani et al., 2021). Consistent with our findings, the cluster displaying predominant tibial adduction exhibited greater internal rotation, while the cluster with predominant tibial abduction demonstrated relatively more external rotation. Similarly, Zgolli et al. identified two clusters in 165 healthy knees, noting significant differences in adduction/abduction and internal/external rotation (Zgolli et al., 2018). However, specific orientations were not described, complicating direct comparison. Notably, cluster analysis based on PF kinematics has not been reported in the existing literature. It is important to highlight that, based on cluster analysis alone, it is not possible to establish causal relationships between kinematic variables. While our findings suggest an association between tibial adduction, tibial internal rotation, lateral patellar translation and tilt, we are not able to draw conclusions regarding causal relationships between these specific parameters. As such, cluster analysis provides valuable insights into kinematic phenotypes, but further research is necessary to determine the clinical implications of kinematic associations.

This study is the first to analyze kinematic patterns using a clustering approach based on dynamic CT imaging data. Our results provide novel insights into healthy TF and PF kinematics during knee flexion and extension. Dynamic CT has the potential to be incorporated into clinical workflows for assessing knee kinematics, making it accessible to all patients. Another strength of this study lies in the application of SPM analysis, enabling comprehensive statistical analysis across the entire range of motion while minimizing the risk of associated false hypothesis testing and bias (Pataky et al., 2013; Pataky et al., 2015). However, some limitations should also be considered. First, this study analyzed bilateral CT data exclusively from Caucasian individuals, primarily females, with an average age of 24.4 years, which may limit the generalizability of our findings. Nevertheless, this study population was deliberately chosen to represent patients typically affected by PF instability, predominantly young females (Fithian et al., 2004; Zheng et al., 2022). Additionally, we assessed the influence of using bilateral data on the clustering output. Sensitivity analyses including unilateral knees only resulted in < 1 % difference in clustering output, showing our bilateral results to be robust. Furthermore, the definition of the CS used in this study may influence knee kinematics, particularly for PF kinematics (Kedgley et al., 2015; Lenz et al., 2008). As such, the presented results are specific to this study and may deviate from others using alternative CS definitions. Besides, anatomical variations may affect PF kinematics, as the patella lacks distinct anatomical landmarks for consistent determination of the patellar CS (Dunning et al., 2022; Morton et al., 2007). While statistically significant differences between the clusters were observed for all PF kinematic parameters, future investigations should explore whether these differences correlate with PF morphometry. Last, kinematic data were acquired during active, non-weightbearing knee movement, which might not accurately represent everyday activities like walking, running or squatting (Draper et al., 2011; Esfandiarpour et al., 2018). However, several studies suggest that TF and PF kinematics are more distinct in non-weightbearing conditions, likely because the effects of small, but important ligaments and structures in the knee become more pronounced (Draper et al., 2011; Powers et al., 2003; Victor et al., 2010). This indicates that non-weightbearing assessment may provide alternative insights into subtle knee kinematics, complementing weightbearing analyses, which may evaluate different functional aspects of knee motion. Dynamic CT, as demonstrated by Buzatti et al., enables both non-weightbearing and weight-bearing analyses, offering valuable opportunities for future research in this area (Buzzatti et al., 2023).

Knee kinematics derived from dynamic CT scans were not adjusted for anatomical differences, including variations in shape and size of the bones. Given the heterogeneous morphology of the natural knee joint, these variations could introduce discrepancies in translation values across participants. For instance, male knees typically have larger dimensions than females, potentially resulting in greater translation values (Asseln et al., 2018; Conley et al., 2007; Dargel et al., 2011). This may have influenced our results, as we found a statistically significant difference between clusters for participant height. Additionally, research indicates that knee joint shape varies not only by gender, but also by morphotype and ethnicity, contributing to interindividual variability (Bellemans et al., 2010; Kim et al., 2017). Understanding the association between knee shape and function is crucial for predicting patient-specific knee kinematics. Previous studies have explored this relationship, revealing associations between various anatomical features and kinematics. For instance, tibial tuberosity position and trochlear groove geometry are related to lateral patellar tilt and translation, both in healthy knees and knees with patellar instability (Elias et al., 2016; Varadarajan et al., 2010). Additionally, the shape of the medial femoral condyle influences tibial internal/external rotation, while the slope of the medial tibial plateau and the shape of the lateral femoral condyle are associated with tibial AP translation during gait (Hodel et al., 2022). However, the applicability of these relationships to the two kinematic

phenotypes identified in this study remains uncertain, warranting further investigation in future research.

In conclusion, this study employed K-means clustering to identify two distinct kinematic phenotypes from a comprehensive dataset of healthy knee kinematics obtained through dynamic CT imaging. The two clusters exhibited statistically significant differences in both TF and PF kinematics, particularly evident in internal/external and adduction/abduction rotation of the tibia. The identified kinematic phenotypes underscore the natural variability in healthy knee function and provide valuable insights into the nuanced variations within a healthy population. These findings provide a critical foundation for future studies aimed at improving diagnostic and therapeutic approaches for PF instability using dynamic CT imaging. Future research should explore the association between knee joint morphometry and kinematics. Understanding this association could enable the prediction of personalized knee kinematics based on individual anatomical characteristics, which holds promising implications for patients with PF instability. Anticipating kinematic deviations from established clusters could aid in personalized diagnostics and treatment planning for this pathology. Ultimately, this study highlights the importance of dynamic CT imaging in advancing our understanding of knee kinematics and its potential clinical applications in personalized healthcare.

CRediT authorship contribution statement

E.H.S. Teule: Writing - Original Draft, Conceptualization, Methodology, Software, Validation, Formal analysis, Investigation, Data Curation, Visualization, Project administration. **S.A.W. van de Groes:** Writing - review & editing, Validation, Supervision, Resources, Methodology, Investigation, Data curation, Conceptualization. **G. Hannink:** Writing – review & editing, Validation, Software, Methodology, Investigation, Formal analysis. **N. Verdonschot:** Writing – review & editing, Validation, Supervision, Resources, Methodology, Investigation, Formal analysis, Conceptualization. **D. Janssen:** Writing – review & editing, Validation, Supervision, Resources, Methodology, Investigation, Data curation, Conceptualization.

Declaration of competing interest

The authors declare that they have no known competing financial interests or personal relationships that could have appeared to influence the work reported in this paper.

Acknowledgements

None.

Appendix A. Supplementary material

Supplementary data to this article can be found online at https://doi.org/10.1016/j.jbiomech.2024.112402.

References

Abid, M., Mezghani, N., Mitiche, A., 2019. Knee joint biomechanical gait data classification for knee pathology assessment: a literature review. Appl. Bionics Biomech. 2019, 7472039. https://doi.org/10.1155/2019/7472039.

Abiodun, M.I., Absalom, E.E., Laith, A., Belal, A., Jia, H., 2023. K-means clustering algorithms: a comprehensive review, variants analysis, and advances in the era of big data. Inf. Sci. 622, 178–210. https://doi.org/10.1016/j.ins.2022.11.139.

Adachi, T., Kato, Y., Kiyotomo, D., Kawamukai, K., Takazawa, S., Suzuki, T., Machida, Y., 2023. Accuracy verification of four-dimensional CT analysis of knee joint movements: a pilot study using a knee joint model and motion-capture system. Cureus 15 (2), e35616.

Asseln, M., Hanisch, C., Schick, F., Radermacher, K., 2018. Gender differences in knee morphology and the prospects for implant design in total knee replacement. Knee 25 (4), 545–558. https://doi.org/10.1016/j.knee.2018.04.005.

Barrios, J.A., Heitkamp, C.A., Smith, B.P., Sturgeon, M.M., Suckow, D.W., Sutton, C.R., 2016. Three-dimensional hip and knee kinematics during walking, running, and single-limb drop landing in females with and without genu valgum. Clin. Biomech. (Bristol, Avon) 31, 7–11. https://doi.org/10.1016/j.clinbiomech.2015.10.008.

Bellemans, J., Carpentier, K., Vandenneucker, H., Vanlauwe, J., Victor, J., 2010. The John insall award: both morphotype and gender influence the shape of the knee in patients undergoing TKA. Clin. Orthop. Relat. Res. 468 (1), 29–36. https://doi.org/10.1007/s11999-009-1016-2.

Buzzatti, L., Keelson, B., Vanlauwe, J., Buls, N., De Mey, J., Vandemeulebroucke, J., Cattrysse, E., Scheerlinck, T., 2021. Evaluating lower limb kinematics and pathology with dynamic CT. Bone Joint J 103, 822–827. https://doi.org/10.1302/0301-620X.103B5.BJJ-2020-1064.R2.

Buzzatti, L., Keelson, B., van der Voort, J.W., Segato, L., Scheerlinck, T., Hereus, S., Van Gompel, G., Vandemeulebroucke, J., De Mey, J., Buls, N., Cattrysse, E., Serrien, B., 2023. Dynamic CT scanning of the knee: Combining weight bearing with real-time motion acquisition. Knee 44, 130–141. https://doi.org/10.1016/j.knee.2023.07.014.

Caliński, T., Harabasz, J., 1974. A dendrite method for cluster analysis. Comm. Statist. Simulation Comput. 3 (1), 1–27. https://doi.org/10.1080/03610927408827101.

Chen, H., Kluijtmans, L., Bakker, M., Dunning, H., Kang, Y., van de Groes, S., Sprengers, A.M.J., Verdonschot, N., 2020. A robust and semi-automatic quantitative measurement of patellofemoral instability based on four dimensional computed tomography. Med. Eng. Phys. 78, 29–38. https://doi.org/10.1016/j.medengphy.2020.01.012.

Clement, J., Toliopoulos, P., Hagemeister, N., Desmeules, F., Fuentes, A., Vendittoli, P.A., 2018. Healthy 3D knee kinematics during gait: differences between women and men, and correlation with x-ray alignment. Gait Posture 64, 198–204. https://doi.org/10.1016/j.gaitpost.2018.06.024.

Conley, S., Rosenberg, A., Crowninshield, R., 2007. The female knee: anatomic variations. J. Am. Acad. Orthop. Surg. 15 (Suppl 1), S31–S36. https://doi.org/10.5435/00124635-200700001-00009.

Dandu, N., Knapik, D.M., Trasolini, N.A., Zavras, A.G., Yanke, A.B., 2022. Future directions in patellofemoral imaging and 3D modeling. Curr. Rev. Musculoskelet. Med. 15 (2), 82–89. https://doi.org/10.1007/s12178-022-09746-7.

Dargel, J., Michael, J.W., Feiser, J., Ivo, R., Koebke, J., 2011. Human knee joint anatomy revisited: morphometry in the light of sex-specific total knee arthroplasty. J. Arthroplasty 26 (3), 346–353. https://doi.org/10.1016/j.arth.2009.12.019.

Draper, C.E., Besier, T.F., Fredericson, M., Santos, J.M., Beaupre, G.S., Delp, S.L., Gold, G.E., 2011. Differences in patellofemoral kinematics between weight-bearing and non-weight-bearing conditions in patients with patellofemoral pain. J. Orthop. Res. 29 (3), 312–317. https://doi.org/10.1002/jor.21253.

Dunning, H., van de Groes, S.A.W., Verdonschot, N., Buckens, C.F., Janssen, D., 2022. The sensitivity of an anatomical coordinate system to anatomical variation and its effect on the description of knee kinematics as obtained from dynamic CT imaging. Med. Eng. Phys. 102, 103781. https://doi.org/10.1016/j.medengphy.2022.103781.

Dunning, H., van de Groes, S.A.W., Buckens, C.F., Prokop, M., Verdonschot, N., Janssen, D., 2023. Fully automatic extraction of knee kinematics from dynamic CT imaging; normative tibiofemoral and patellofemoral kinematics of 100 healthy volunteers. Knee 41, 9–17. https://doi.org/10.1016/j.knee.2022.12.011.

Elias, J.J., Soehnlen, N.T., Guseila, L.M., Cosgarea, A.J., 2016. Dynamic tracking influenced by anatomy in patellar instability. Knee 23 (3), 450–455. https://doi.org/10.1016/j.knee.2016.01.021.

Esfandiarpour, F., Lebrun, C.M., Dhillon, S., Boulanger, P., 2018. In-vivo patellar tracking in individuals with patellofemoral pain and healthy individuals. J. Orthop. Res. https://doi.org/10.1002/jor.23887.

Fithian, D.C., Paxton, E.W., Stone, M.L., Silva, P., Davis, D.K., Elias, D.A., White, L.M., 2004. Epidemiology and natural history of acute patellar dislocation. Am. J. Sports Med. 32 (5), 1114–1121. https://doi.org/10.1177/0363546503260788.

Gale, T., Anderst, W., 2020. Knee kinematics of healthy adults measured using biplane radiography. J. Biomech. Eng. 142 (10). https://doi.org/10.1115/1.4047419.

Grood, E.S., Suntay, W.J., 1983. A joint coordinate system for the clinical description of three-dimensional motions: application to the knee. J. Biomech. Eng. 105 (2), 136–144. https://doi.org/10.1115/1.3138397.

Hodel, S., Postolka, B., Flury, A., Schutz, P., Taylor, W.R., Vlachopoulos, L., Fucentese, S. F., 2022. Influence of bone morphology on in vivo tibio-femoral kinematics in healthy knees during gait activities. J Clin Med 11 (17). https://doi.org/10.3390/jcm11175082.

Kedgley, A.E., McWalter, E.J., Wilson, D.R., 2015. The effect of coordinate system variation on in vivo patellofemoral kinematic measures. Knee 22 (2), 88–94. https://doi.org/10.1016/j.knee.2014.11.006.

Kim, T.K., Phillips, M., Bhandari, M., Watson, J., Malhotra, R., 2017. What differences in morphologic features of the knee exist among patients of various races? A systematic review. Clin. Orthop. Relat. Res. 475 (1), 170–182. https://doi.org/10.1007/s11999-016-5097-4.

Lenz, N.M., Mane, A., Maletsky, L.P., Morton, N.A., 2008. The effects of femoral fixed body coordinate system definition on knee kinematic description. J. Biomech. Eng. 130 (2), 021014. https://doi.org/10.1115/1.2898713.

Li, X., Chen, H., Qi, X., Dou, Q., Fu, C.W., Heng, P.A., 2018. H-DenseUNet: hybrid densely connected UNet for liver and tumor segmentation from CT volumes. IEEE Trans. Med. Imaging 37 (12), 2663–2674. https://doi.org/10.1109/TMI.2018.2845918.

Lin, Y.F., Jan, M.H., Lin, D.H., Cheng, C.K., 2008. Different effects of femoral and tibial rotation on the different measurements of patella tilting: an axial computed tomography study. J. Orthop. Surg. Res. 3, 5. https://doi.org/10.1186/1749-799X-3-5.

MacQueen, J., 1967. Some methods for classification and analysis of multivariate observations. In: Proceedings of the Fifth Berkeley Symposium on Mathematical

Statistics and Probability (Vol. 1, pp. 281-297). University of California Press, Berkeley.
Mezghani, N., Soltana, R., Ouakrim, Y., Cagnin, A., Fuentes, A., Hagemeister, N., Vendittoli, P.-A., 2021. Healthy knee kinematic phenotypes identification based on a clustering data analysis. Appl. Sci. 11 (24). https://doi.org/10.3390/app112412054.
Miranda, D.L., Rainbow, M.J., Leventhal, E.L., Crisco, J.J., Fleming, B.C., 2010. Automatic determination of anatomical coordinate systems for three-dimensional bone models of the isolated human knee. J. Biomech. 43 (8), 1623–1626. https://doi.org/10.1016/j.jbiomech.2010.01.036.
Morton, N.A., Maletsky, L.P., Pal, S., Laz, P.J., 2007. Effect of variability in anatomical landmark location on knee kinematic description. J. Orthop. Res. 25 (9), 1221–1230. https://doi.org/10.1002/jor.20396.
Pataky, T.C., 2017. Power1D: a Python toolbox for numerical power estimates in experiments involving one-dimensional continua. PeerJ Comput. Sci. 3, e125. https://doi.org/10.7717/peerj-cs.125.
Pataky, T.C., Robinson, M.A., Vanrenterghem, J., 2013. Vector field statistical analysis of kinematic and force trajectories. J. Biomech. 46 (14), 2394–2401. https://doi.org/10.1016/j.jbiomech.2013.07.031.
Pataky, T.C., Vanrenterghem, J., Robinson, M.A., 2015. Zero- vs. one-dimensional, parametric vs. non-parametric, and confidence interval vs. hypothesis testing procedures in one-dimensional biomechanical trajectory analysis. J. Biomech. 48 (7), 1277–1285. https://doi.org/10.1016/j.jbiomech.2015.02.051.
Petersen, E.T., Rytter, S., Koppens, D., Dalsgaard, J., Hansen, T.B., Larsen, N.E., Andersen, M.S., Stilling, M., 2022. Patients with knee osteoarthritis can be divided into subgroups based on tibiofemoral joint kinematics of gait - an exploratory and dynamic radiostereometric study. Osteoarthritis and Cartilage / Oars, Osteoarthritis Research Society 30 (2), 249–259. https://doi.org/10.1016/j.joca.2021.10.011.
Pinskerova, V., Johal, P., Nakagawa, S., Sosna, A., Williams, A., Gedroyc, W., Freeman, M.A., 2004. Does the femur roll-back with flexion? J. Bone Joint Surg. Brit. 86 (6), 925–931. https://doi.org/10.1302/0301-620x.86b6.14589.
Powers, C.M., Ward, S.R., Fredericson, M., Guillet, M., Shellock, F.G., 2003. Patellofemoral kinematics during weight-bearing and non-weight-bearing knee extension in persons with lateral subluxation of the patella: a preliminary study. J. Orthop. Sports Phys. Ther. 33 (11), 677–685. https://doi.org/10.2519/jospt.2003.33.11.677.
Rosa, S.B., Ewen, P.M., Doma, K., Ferrer, J.F.L., Grant, A., 2019. Dynamic evaluation of patellofemoral instability: a clinical reality or just a research field? A literature review. Orthopaedic Surgery 11 (6), 932–942. https://doi.org/10.1111/os.12549.
Rousseeuw, P.J., 1987. Silhouettes: A graphical aid to the interpretation and validation of cluster analysis. J. Comput. Appl. Math. 20, 53–65. https://doi.org/10.1016/0377-0427(87)90125-7.
Santos, J. M., & Embrechts, M. (2009, 2009//). On the Use of the Adjusted Rand Index as a Metric for Evaluating Supervised Classification. Artificial Neural Networks – ICANN 2009, Berlin, Heidelberg.
Shen, A., Boden, B.P., Grant, C., Carlson, V.R., Alter, K.E., Sheehan, F.T., 2021. Adolescents and adults with patellofemoral pain exhibit distinct patellar maltracking patterns. Clin. Biomech. (Bristol, Avon) 90, 105481. https://doi.org/10.1016/j.clinbiomech.2021.105481.
Tanaka, M.J., Elias, J.J., Williams, A.A., Demehri, S., Cosgarea, A.J., 2016. Characterization of patellar maltracking using dynamic kinematic CT imaging in patients with patellar instability. Knee Surg. Sports Traumatol. Arthrosc. 24 (11), 3634–3641. https://doi.org/10.1007/s00167-016-4216-9.
Varadarajan, K.M., Freiberg, A.A., Gill, T.J., Rubash, H.E., Li, G., 2010. Relationship between three-dimensional geometry of the trochlear groove and in vivo patellar tracking during weight-bearing knee flexion. J. Biomech. Eng. 132 (6), 061008. https://doi.org/10.1115/1.4001360.
Victor, J., Labey, L., Wong, P., Innocenti, B., Bellemans, J., 2010. The influence of muscle load on tibiofemoral knee kinematics. J. Orthop. Res. 28 (4), 419–428. https://doi.org/10.1002/jor.21019.
Wong, M.T., Wiens, C., Kuczynski, M., Manske, S., Schneider, P.S., 2022. Four-dimensional computed tomography: musculoskeletal applications. Canadian Journal of Surgery. Journal Canadien de Chirurgie 65 (3), E388–E393. https://doi.org/10.1503/cjs.023420.
Yu, Z., Yao, J., Wang, X., Xin, X., Zhang, K., Cai, H., Fan, Y., Yang, B., 2019. Research Methods and progress of patellofemoral joint kinematics: a review. J. Healthcare Engi. 2019, 9159267. https://doi.org/10.1155/2019/9159267.
Zgolli, F., Henni, K., Haddad, R., Mitiche, A., Ouakrim, Y., Hagemeister, N., Vendittoli, P. A., Fuentes, A., & Mezghani, N., 2018, 13-12-2018. Kinematic Data Clustering for Healthy Knee Gait Characterization IEEEE Life Sciences Conference, Montreal, QC, Canada. https://ieeexplore.ieee.org/stampPDF/getPDF.jsp?tp=&arnumber=8572119&ref=.
Zheng, E.T., Kocher, M.S., Wilson, B.R., Hussain, Z.B., Nunally, K.D., Yen, Y.M., Kramer, D.E., Micheli, L.J., Heyworth, B.E., 2022. Descriptive epidemiology of a surgical patellofemoral instability population of 492 patients, 23259671221108174 Orthop J Sports Med 10 (7). https://doi.org/10.1177/23259671221108174.